

Stratigraphic sequence, elemental concentrations and heavy metal pollution in Holocene sediments from the Tinto-Odiel Estuary, southwestern Spain

F. Ruiz · M. L. González-Regalado · J. Borrego · J. A. Morales · J. G. Pendón
J. M. Muñoz

Abstract The Holocene filling of the Tinto-Odiel Estuary comprises seven lithofacies over a Mio-Pliocene substrate. The sequence includes three system tracts: lowstand system (10 000 to 8700 years BP), transgressive system (8700 to 7000 years BP), and regressive system (7000 to Recent). Twenty sediment samples from the 50-m borehole were analyzed for their major components and minor element concentrations. Two multivariate analysis methods, principal component analysis and cluster analysis, were performed in the analytical data set to help visualize the sample clusters and the element associations. Samples corresponding to unpolluted, pre-mining sediments are clearly separated by cluster analysis, mainly as a result of the low content in sulphide-associated heavy metals such as Cu, Zn, As, Ag, and Pb. So, these sediments may be utilized as a background for geochemical analysis (bulk sample) in other adjacent estuaries, both in sandy and silty-clayey sediments. As a consequence of large-scale mining and smelting operations occurred since prehistoric times on the river banks, a rapid rise in the metal pollution was found in the upper 2.5 m of the natural filling, with values exceeding up to ten times the natural background levels. In addition, since the mid-1960s,

large amounts of waste and pollutant effluents have been discharged from industries located around the estuary, increasing the heavy metal content in the last 0.3 m of the natural sedimentation.

Key words Estuaries · Holocene record · Depositional environment · Background · Metallic pollution · Mine waste contamination · Anthropogenic discharge

Introduction

The Tinto-Odiel estuary is one of the most polluted zones in southwestern Europe. The sources of this pollution include: (1) large amounts of suspended material carried from northern Huelva province, one of the most important mining areas in western Europe, with Cu, Zn, Pb, Au, and Ag ore bodies. In the mining history of this mineralized district, the so-called Iberian Pyrite Belt, some phases may be distinguished, with minor activity during the interacts. In the Iberian (5000 to 6000 years BP), Phoenician (2800 to 2600 years BP) and Roman (2000 and 1800 years BP) phases, numerous Ag-Au deposits were extensively mined, being posteriorly abandoned by the Visigoths (1600 to 1300 years BP) and Arabs (1300 to 500 years BP) (Blanco Freijero and Rothenberg 1981; Ferrero 1988). The pyrite production peaked between 1875 and 1930 and, at present, only some mines (Riotinto, Tharsis) are still working. (2) Since 1960, wastes containing high levels of heavy metals were discharged from vast industrial concentrations (alkalines, fertilizers, metallurgics) in the estuarine border. (3) Urban effluents. As a consequence of both acid mine-drainage and industrial waste dumping, recent estuarine sediments at the Tinto-Odiel junction contain concentration levels of toxic metals as high as (in mg/kg dry wt, fraction < 63 μm): 4500–6300 Cu; 2600–5100 Zn; 1900–3400 As; 1700–10 400

Received: 18 August 1997 · Accepted: 19 January 1998

F. Ruiz (✉) · M. L. González-Regalado
J. Borrego · J. A. Morales · J. G. Pendón
Departamento de Geología, Universidad de Huelva,
E-21819-Palos de la Frontera, Huelva, Spain
Tel.: +34 5935 1000 · Fax: +34 59530175
e-mail: montero@uhu.es

J. M. Muñoz
Departamento de Estadística e Investigación Operativa,
Universidad de Sevilla, E-41071 Sevilla, Spain

Pb; 200–700 Mn; 9–39 Cd; and 15–49 Hg, in accordance with data of Pérez and others (1991), Cabrera and others (1992), and Nelson and Lamothe (1993). Although it is difficult to distinguish between pollution resulting from mining activities and contamination of an industrial origin, Serrano and others (1995) estimated that the concentration of heavy metals in the Huelva estuary has the following provenance: 83% is supplied by the acid mine-drainage; 16.9% has an industrial origin; and 0.1% has its source in the urban effluents. Nevertheless, some surveys of the Andalucía Board (A.M.A. 1994) indicate that 60–80% of heavy metal pollution has an industrial origin. Since 1985, this zone is subject of a Corrective Plan for Control of industrial Waste Disposal.

The aims of this paper are: (1) to analyze the changes produced in the sedimentological and geochemical features of estuarine sediments during the Holocene; (2) to place these changes in a chronological sequence based upon radiocarbon dating (corrected radiocarbon ages) and historical data; and (3) to obtain a geochemical background for the Tinto-Odiel Estuary.

The Tinto-Odiel Estuary

The Tinto-Odiel Estuary is a 25-km-long incised valley on the southwestern coast of Spain, underlain by Neogene sandy-silty sediments. Borrego (1992) delimited three domains in the estuary (Fig. 1): (1) High Estuary, characterized by a braided channel system; (2) Middle Estuary, with three distributary channels cutting elongated salt-marsh bodies (i.e., the Bacuta Island) in which vegetation is dominated by species tolerant of variable salinity such as *Sarcocornia fruticosa* and *Spartina densiflora* (Rubio 1985); and (3) Marine Estuary, which is composed by a central salt-marsh body (Saltés Island) located between the main channels and protected by sandy barriers. Fluvial discharge and tidal regime are the fundamental hydrodynamic processes in the Huelva Estuary. The freshwater discharge of the Tinto and Odiel Rivers is subject to seasonal changes. The highest runoff occurs from December to February in both streams (an average of 100 hm³/month), and the lowest runoff occurs during the summer months (<1 hm³/month). The tidal regime is

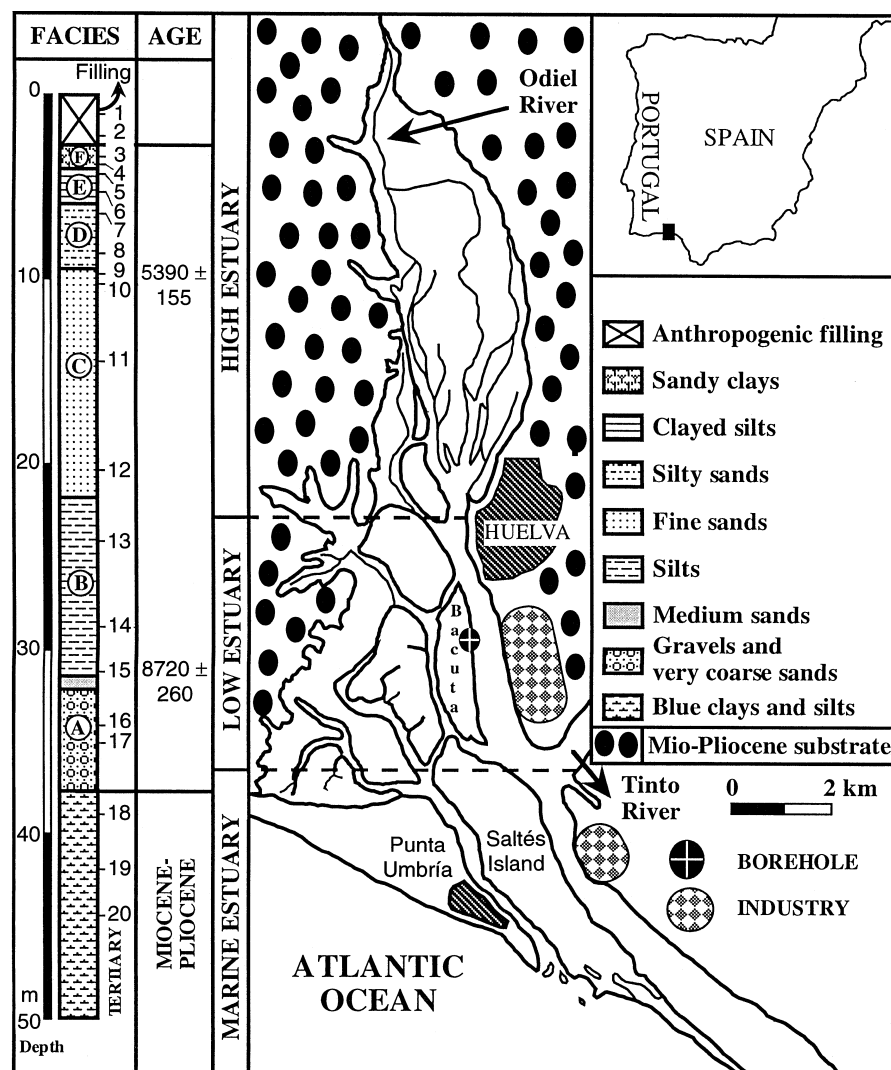


Fig. 1 Map of the Tinto-Odiel Estuary showing the location of the borehole

Table 1
Granulometric data of sediment samples

Sam- ples	gravel (>2 mm)	sand				silt				clay (<4 µm)	
		very coarse 2– 1 mm	coarse 1– 0.5 mm	medium 0.5– 0.25 mm	fine 0.25– 0.125 mm	very fine 0.125– 0.063 mm	coarse 63– 32 µm	medium 32– 16 µm	fine 16– 8 µm		very fine 8– 4 µm
1	1.8	1.4	1.1	1.9	4.8	4.3	9.1	14.1	21.9	24.4	15.2
2	1.2	1.0	1.1	6.5	8.9	6.2	2.1	7.2	21.4	28.6	15.8
3	3.1	2.1	1.9	2.5	3.7	2.9	3.1	12.4	24.2	28.0	16.2
4	0.4	0.3	0.2	0.4	0.5	0.4	1.6	9.2	29.2	38.0	19.8
5	0.2	0.3	0.3	0.4	0.4	0.5	11.6	17.4	25.8	28.4	14.7
6	0.3	0.1	0.3	0.6	2.1	19.0	7.2	16.0	20.8	21.6	12.2
7	0.4	0.5	0.5	0.6	4.4	47.5	6.6	10.0	11.9	11.3	6.2
8	0.2	0.2	0.2	0.4	9.7	43.8	1.8	10.0	13.0	12.1	8.6
9	7.2	5.3	4.1	30.0	22.4	16.6	0.8	3.4	4.5	3.6	2.1
10	0.4	0.3	1.7	39.6	14.3	27.9	0.0	3.2	5.6	4.1	3.0
11	0.3	0.1	1.3	19.7	34.5	12.0	4.6	8.4	9.1	6.6	3.3
12	0.0	0.2	0.6	26.2	32.6	6.2	0.0	7.3	11.0	9.7	6.3
13	0.1	0.2	0.2	0.7	2.1	5.6	11.8	19.7	24.8	23.3	11.6
14	0.2	0.3	0.3	0.4	1.7	14.8	12.2	17.6	21.5	20.4	10.5
15	6.2	3.8	6.6	19.9	14.0	3.9	3.7	8.6	14.0	12.3	6.9
16	31.2	7.8	5.9	17.1	4.4	11.6	3.2	5.3	6.0	5.0	2.5
17	26.8	9.8	8.8	7.7	6.4	5.7	6.9	8.3	8.7	7.4	3.7
18	0.9	0.3	0.6	1.1	1.6	5.7	22.3	24.0	21.1	16.0	6.5

Table 2
Chemical analysis of nine major elements and LOI (loss in ignition) for 20 sediment samples

% analytical error	SiO ₂ 0.01	Al ₂ O ₃ 0.01	Fe ₂ O ₃ 0.01	MnO 0.01	CaO 0.01	TiO ₂ 0.001	K ₂ O 0.01	Na ₂ O 0.01	MgO 0.01	P ₂ O ₅ 0.01	LOI 0.01
1	48.3	15.90	14.30	0.06	1.20	0.86	2.20	1.68	1.65	0.17	13.60
2	65.4	10.10	10.40	0.05	1.32	0.69	1.59	1.52	1.26	0.09	7.65
3	45.9	13.80	16.60	0.10	1.41	0.76	2.04	2.18	1.62	0.17	15.50
4	52.4	18.70	7.63	0.05	1.02	1.01	3.00	2.04	2.09	0.15	12.20
5	52.9	17.20	7.57	0.05	0.87	0.97	2.91	2.18	2.14	0.11	13.40
6	65.6	11.80	4.96	0.04	2.17	0.78	2.25	1.99	1.50	0.08	9.05
7	72.3	9.71	3.52	0.03	2.39	0.68	1.90	1.94	1.17	0.06	6.55
8	74.2	8.30	2.97	0.03	3.16	0.59	1.71	1.69	0.98	0.07	6.10
9	71.7	3.81	1.72	0.02	10.20	0.36	0.77	0.74	0.42	0.04	9.85
10	86.7	3.44	1.19	0.01	3.01	0.26	1.02	0.74	0.32	0.04	3.55
11	86.9	4.23	1.27	0.01	1.96	0.31	1.26	0.78	0.37	0.04	2.95
12	90.6	2.57	0.71	0.05	1.90	0.16	0.89	0.54	0.22	0.03	2.50
13	58.4	12.40	5.19	0.04	5.88	0.71	2.10	1.50	1.94	0.11	11.90
14	58.6	11.50	4.72	0.04	6.76	0.72	2.04	1.55	1.85	0.10	12.30
15	66.1	9.65	4.26	0.05	6.53	0.58	1.72	1.03	1.21	0.06	8.95
16	88.3	4.49	2.50	0.03	0.68	0.23	0.79	0.87	0.49	0.06	1.65
17	89.5	4.03	2.51	0.02	0.44	0.19	0.58	0.84	0.54	0.05	1.45
18	52.2	9.07	4.79	0.08	12.70	0.60	1.35	1.00	2.42	0.14	16.00
19	44.7	10.30	4.41	0.04	15.70	0.64	1.54	1.04	2.67	0.12	19.20
20	43.5	11.70	5.35	0.05	15.40	0.69	1.93	0.81	2.74	0.15	17.90

mesotidal (mean range 2.15 m) and semidiurnal with a low diurnal amplitude (Borrego and others 1993). Under average discharge conditions, mixing in the Huelva estuary is controlled by the tidal prism. The estuary is well-mixed during spring tides (35–36‰) and becomes partially stratified during the rainy season, the brackish wa-

ter (2–14‰) flowing seaward over a lower, saltier layer (29–32‰) (I.E.O. 1992).

In recent years a significant improvement of the water quality has been determined. In 1981 and 1982, high concentrations of sulphates and Zn were detected in the acid waters (pH = 2–5) of the estuary (I.E.O. 1982; M.O.P.U.

Table 3
Chemical analysis of trace elements (in mg/kg) in sediments of the borehole

mg/kg analytical error	Be	Sc	V	Cr	Co	Ni	Cu	Zn	As	Sr	Y	Zr	Mo	Ag	Ba	Pb
	0.5	0.5	2	1	1	1	0.5	0.5	3	0.5	0.1	0.5	1	0.2	1	2
1	1.4	6	62	42	10	18	933	858	531	28.1	10.6	7.9	9	0.8	485	175
2	1	3.1	39	23	8	11	767	720	440	21.8	7.2	5.3	8	1.7	418	164
3	1.5	5.3	59	38	15	18	906	1370	697	38.1	12.9	7.7	11	1.8	491	234
4	1.5	7	65	48	18	28	175	412	63	24.6	12.1	9	6	0.8	69	81
5	1.3	5.1	54	39	14	24	278	170	50	26.0	9.8	8	3	1.1	38	101
6	0.8	2.7	30	23	9	14	18.8	47.3	13	37.3	6.4	7.8	3	0.5	24	16
7	0.6	2.1	24	19	5	9	15.6	38.1	4	43.0	5.2	6.1	2	0.6	25	13
8	0.6	1.9	21	17	6	8	8.1	29.4	8	86.0	4.8	5.2	2	<0.2	20	6
9	<0.5	0.8	13	8	4	4	6.1	14.4	<3	317	2.5	3.7	2	0.7	14	11
10	<0.5	<0.5	8	6	4	2	10.3	12.5	12	82.9	1.9	3	<1	0.5	13	2
11	<0.5	0.6	11	7	3	3	4.5	10.5	6	54.2	2.3	4.2	3	0.3	15	5
12	<0.5	<0.5	6	5	3	<1	3.8	6.3	<3	58.5	1.4	3.4	<1	<0.2	15	<2
13	1	2.9	31	23	8	15	19.4	39.9	<3	107	6.9	8.1	1	0.5	35	51
14	0.9	2.7	30	22	7	13	12.6	35.8	11	130	6.6	7.9	2	0.5	28	18
15	0.7	2.3	23	18	9	11	11.8	41.7	4	151	5.6	6.6	<1	0.3	20	14
16	<0.5	0.9	13	13	5	8	14.2	24.6	7	9.4	2.9	4.6	2	0.2	14	4
17	<0.5	1	14	12	6	8	40	27.3	13	6.8	2.7	4.6	2	0.5	18	3
18	0.7	2.8	23	23	5	12	8.5	37.7	10	205	7.4	6.1	<1	0.8	28	5
19	0.7	2.7	21	21	6	13	10	38.5	5	243	7.3	5.5	1	<0.2	32	9
20	0.8	3.2	22	24	6	17	12.4	42.5	9	259	8.2	5.8	1	0.4	38	7

1982). In April 1991, waters were even neutral (pH = 6.61–7.36) during high tides, both on the surface and in the bottom layers (I.E.O. 1992).

Methods

The Bacuta Island, located near the confluence of the Tinto and Odiel Rivers, was selected by the CEDEX (a division of the Spanish Industry Ministry) for recovering a continuous 50-m core. Twenty samples were taken and divided into two or three subsamples.

Grain size analysis

The subsamples for grain size (50 g) were sifted through sieves with a screen between 2 and 0.063 μm . The clayed-silty fraction was then run on a Coulter Counter utilizing a 100- μm tube and an analysis range of between 2 and 70 μm .

Metal analysis

Chemical analysis for major elements and trace metals in sediment were performed on the bulk samples by X-Ray Assay Laboratories, Toronto (Canada). Metal concentrations were determined by X-Ray Fluorescence (SiO_2 , Al_2O_3 , Fe_2O_3 , MnO , CaO , TiO_2 , K_2O , Na_2O , P_2O_5) and ICP Mass Spectrometry (Be, Sc, V, Cr, Co, Ni, Cu, Zn, As, Y, Zr, Mo, Ag, Ba, Pb), with previous nitric aqua regia digestion. The calibration is based on the analysis of over 40 international standard reference materials. The LOI (loss in ignition) calculation was made as the difference

between the sum total of major and minor elements, and 100%.

Radiocarbon dating

Carbon-14 dating (C-13 corrected, Geochron Laboratories) was performed on two sediment samples (sample 9: reference GX-21287; sample 15: reference GX-21288) with abundant remains of shells, mainly Ostreidae. The shells (15–20 g) were cleaned thoroughly in an ultrasonic cleaner. They were then leached thoroughly with dilute HCl to remove additional surficial material which may have been altered, and to be sure only fresh carbonate material was used. The cleaned shells were then hydrolyzed with HCl, under vacuum, and the carbon dioxide was recovered for analysis.

Statistical analysis

Firstly, a normality test was applied to the data matrix (elements and LOI). Fourteen variables (Ag, As, Ba, Be, CaO, Co, Cu, Fe_2O_3 , Mo, Na_2O , Pb, Sr, V, Zn) are not normally distributed. Consequently, the algorithm after Spearman is used for bivariate analysis.

For multivariate analysis, the variables were row-normalized scaling the raw analytical data of each element to zero mean and unit variance in order to eliminate the effect of differences in magnitude and variance of the data. Two multivariate methods have been used to help data interpretation: (1) cluster analysis [K-means method of Anderberg (1973)] differentiates three clusters; (2) principal component analysis (PCA), with 95.04% of the total variance explained by the four main factors. This percentage explained is recommended by Reyment and Jor-

Table 4
Spearman algorithm matrix

	SiO ₂	Al ₂ O ₃	Fe ₂ O ₃	MnO	CaO	TiO ₂	K ₂ O	MgO	Na ₂ O	P ₂ O ₅	LOI	Be	Sc	V	Cr	Co	Ni	Cu	Zn	As	Sr	Y	Zr	Mo	Ag	Ba	Pb		
SiO ₂	1																												
Al ₂ O ₃	0.78**	1																											
Fe ₂ O ₃	0.81**	0.91**	1																										
MnO	0.67**	0.60**	0.74**	1																									
CaO	0.35-	0.12-	0.13-	0.02-	1																								
TiO ₂	0.75**	0.96**	0.88**	0.55*	0.07-	1																							
K ₂ O	0.63**	0.93**	0.78**	0.52*	0.07-	0.94**	1																						
MgO	0.91**	0.78**	0.76**	0.60**	0.31	0.72**	0.64**	1																					
Na ₂ O	0.47*	0.81**	0.73**	0.42	0.83**	0.83**	0.81**	0.50*	1																				
P ₂ O ₅	0.92**	0.86**	0.90**	0.73**	0.80**	0.80**	0.70**	0.88**	0.63**	1																			
LOI	0.97**	0.68**	0.69**	0.63**	0.48*	0.68**	0.56**	0.88**	0.39	0.84**	1																		
Be	0.79**	0.94**	0.96**	0.73**	0.07-	0.93**	0.88**	0.74**	0.77**	0.87**	0.69**	1																	
Sc	0.85**	0.93**	0.98**	0.75**	0.10-	0.89**	0.80**	0.83**	0.71**	0.94**	0.74**	0.96**	1																
V	0.67**	0.92**	0.93**	0.65**	0.22-	0.93**	0.86**	0.65**	0.85**	0.79**	0.56**	0.95**	0.92**	1															
Cr	0.83**	0.95**	0.96**	0.72**	0.11-	0.92**	0.84**	0.83**	0.75**	0.93**	0.74**	0.94**	0.99**	0.92**	1														
Co	0.60**	0.88**	0.86**	0.60**	0.28-	0.83**	0.81**	0.59**	0.81**	0.73**	0.48*	0.90**	0.85**	0.90**	0.84**	1													
Ni	0.84**	0.98**	0.91**	0.66**	0.92**	0.92**	0.87**	0.86**	0.74**	0.91**	0.76**	0.95**	0.96**	0.89**	0.97**	0.87**	1												
Cu	0.41-	0.73**	0.79**	0.43	0.57*	0.68**	0.60**	0.39	0.69**	0.60**	0.24	0.74**	0.74**	0.82**	0.74**	0.80**	0.70**	1											
Zn	0.75**	0.89**	0.96**	0.71**	0.17-	0.85**	0.78**	0.68**	0.76**	0.82**	0.62**	0.92**	0.88**	0.92**	0.92**	0.90**	0.68**	0.81**	1										
As	0.38-	0.52*	0.66**	0.41	0.51*	0.56**	0.43	0.30	0.55*	0.55*	0.25	0.60**	0.61**	0.61**	0.63**	0.54*	0.73**	0.64**	0.58**	1									
Sr	0.29-	0.19-	0.21-	0.01-	0.96**	0.14-	0.12-	0.21	0.37-	0.00	0.45*	0.17-	0.16-	0.30	0.18-	0.33-	0.12-	0.65**	0.25-	0.58**	1								
Y	0.91**	0.90**	0.95**	0.77**	0.02-	0.85**	0.75**	0.87**	0.70**	0.97**	0.82**	0.92**	0.87**	0.87**	0.96**	0.80**	0.95**	0.67**	0.90**	0.59**	0.08-	1							
Zr	0.65**	0.92**	0.79**	0.56**	0.06-	0.89**	0.91**	0.74**	0.79**	0.75**	0.59**	0.87**	0.78**	0.90**	0.86**	0.84**	0.74**	0.64**	0.79**	0.37	0.12-	0.79**	1						
Mo	0.21-	0.54*	0.57**	0.18	0.59**	0.58**	0.45*	0.09	0.63**	0.38	0.10	0.53*	0.51*	0.61**	0.52*	0.55*	0.45*	0.67**	0.57*	0.68**	0.62**	0.45*	0.37	1					
Ag	0.43-	0.46	0.67**	0.45*	0.30-	0.60**	0.41	0.31	0.50*	0.47*	0.37	0.62**	0.62**	0.71**	0.63**	0.51*	0.52*	0.69**	0.62**	0.64**	0.32-	0.59**	0.46*	0.57**	1				
Ba	0.83**	0.87**	0.96**	0.76**	0.08-	0.83**	0.74**	0.77**	0.69**	0.90**	0.71**	0.93**	0.95**	0.88**	0.92**	0.78**	0.87*	0.71**	0.90**	0.58**	0.15-	0.93**	0.74**	0.52*	0.59**	1			
Pb	0.64**	0.85**	0.87**	0.55**	0.15-	0.87**	0.78**	0.52*	0.78**	0.68**	0.55*	0.90**	0.82**	0.92**	0.81**	0.84**	0.79**	0.75**	0.88**	0.50*	0.19-	0.77**	0.78**	0.68**	0.68**	0.82**	1		

** : > 99%
* : 95%–99%

esko (1993) for this analysis. Factor loadings of up to |0.6| were considered to be significant from statistical analysis. In these analysis, normality is only required if both mathematical prediction or inference are given (not studied in this paper).

Results

Sedimentological and geochemical results are presented in Tables 1, 2, and 3. Table 4 includes the Spearman matrix. Table 5 represents the principal component analysis, with the contributions of the 27 chemical elements on the first four factorial axes. Factor 4 is not significant (low variance explained and low loadings in the variables). Classification of the samples (Table 6) differentiates three clusters with significant probability (<0.05) in all elements and LOI.

Discussion and conclusions

Sedimentological analysis

The lower 12 m of the core comprised massive gray-blue silts and clays with conchoid fracture. This layer is very monotonous and only some sandy laminae were observed near the top. Invertebrates are present within the recovered core, such as echinoids or bivalves. They are Neogene sediments belonging to the Gibraleón Clay Formation (Civis and others 1987). These sedimentary rocks were deposited in a open-bay environment (depth up to 50 m) (Ruiz Muñoz and González-Regalado 1990).

The upper limit of the Neogene materials is formed by an erosional unconformity over which lie 5.6 m of coarse to very coarse sand and gravels with silty matrix (Fig. 1, Facies A), without faunal remains. These first estuarine deposits have a fluvial origin. Similar sediments were found at the base of estuarine sediments in many cores located in other Atlantic estuaries (Dalrymple and others 1992; Allen and Posamentier 1993). Zazo and others (1996) indicate that the estuarine sedimentation began over 10000 years BP in the Atlantic coast of the Cádiz Gulf. The sedimentation rate of these fluvial sediments was 0.43 cm/year between 10000 and 8700 years BP (sample 15).

These coarse sediments are overlain by 11.3 m of very compact gray-green clayey silts (Fig. 1, Facies B), with high percents of medium to fine silts (Table 1). Macrofauna is well represented in the lower part, with bivalves (*Corbula gibba*, *Chamelea gallina*, and *Ostrea edulis*), gastrophods (*Cymbium olla*) or scaphopods (*Dentalium vulgare*). Goy and others (1996) indicate that similar deposits were deposited in a tidal flat (lower part) and an open bay (upper part: 8000 to 7000 years BP) in some adjacent estuaries. These data support a sedimentation rate of 0.66 cm/year between 8700 and 7000 years BP.

At the top, there are 10.4 m of well-sorted loose yellow sands (Fig. 1, Facies C), which are fine sands at the base

and are progressively replaced by medium sands in the last meters. Microfauna is scarce at the base (the marine bivalve *Chamelea gallina*), whereas marine bivalves (*Acanthocardia aculeata*, *Anomia ephippium*) coexist with estuarine gastrophods (*Bittium reticulatum*) near the upper limit. These sands were accumulated (0.65 cm/year) in a partially filled estuary (Goy and others 1996) between 7000 and 5390 years BP (sample 9). The overlying sediments comprise 4 m of very bioturbated gray silty sands (Fig. 1, Facies D) with very fine sands in high proportions (40–50%). There is little microfauna, with a mixture of estuarine species and redeposited marine forms. These features were found in some shallow channels of adjacent estuaries (Borrego and others 1993).

In the next 2 m, there are gray to black clayey silts (Fig. 1, Facies E) with many burrows and some juvenile specimens of bivalves and gastrophods. This facies was found in some intertidal environments of the Huelva coast, such as the channel margin of the main fluvial currents (Borrego and others 1995). The Holocene filling of the Low Estuary is completed by salt-marsh deposits, with red muds that are strongly bioturbated by roots (Fig. 1,

Table 5

Variable loadings on the first four factors from a principal component analysis of chemical composition data

	Factor 1	Factor 2	Factor 3	Factor 4
SiO ₂	0.687-	0.313-	0.650-	0.032-
Al ₂ O ₃	0.948	0.270	0.133	0.009
Fe ₂ O ₃	0.502	0.849	0.091	0.061
MnO	0.521	0.602	0.414	0.018
CaO	0.088-	0.278-	0.951	0.056
TiO ₂	0.919	0.235	0.196	0.172-
K ₂ O	0.958	0.099	0.012	0.127-
MgO	0.707	0.032	0.647	0.103
Na ₂ O	0.806	0.321	0.217-	0.341-
P ₂ O ₅	0.670	0.477	0.446	0.295
LOI	0.563	0.214	0.786	0.030
Be	0.842	0.513	0.101	0.011
Sc	0.863	0.451	0.099	0.139
V	0.810	0.564	0.058-	0.034
Cr	0.881	0.428	0.068	0.134
Co	0.831	0.394	0.135-	0.019
Ni	0.932	0.219	0.138	0.122
Cu	0.220	0.949	0.084-	0.049
Zn	0.260	0.951	0.051-	0.052
As	0.132	0.980	0.036-	0.045
Sr	0.213-	0.266-	0.878	0.091-
Y	0.815	0.507	0.252	0.081
Zr	0.927	0.170	0.050	0.012-
Mo	0.310	0.895	0.199-	0.021
Ag	0.259	0.819	0.010	0.374-
Ba	0.946	0.283	0.017-	0.008-
Pb	0.374	0.909	0.082-	0.040-
variance explained				
	12.922	8.446	3.806	0.487
% variance explained				
	47.861	31.281	14.096	1.803

Facies F). In the last 5400 years, a low sedimentation rate may be deduced (0.11 cm/year).

The last 3 m of the borehole are a package of clayed silts. They correspond to a recent artificial fill from the dredging of the Odiel River and wastes from nearby saltworks. In conclusion, this sequence may be grouped in three system tracts: (1) fluvial gravels and coarse sands (Fig. 1, Facies A) comprise a lowstand system tract (*sensu* Allen and Posamentier 1993) supplied by the Tinto and Odiel Rivers between 10000 and 8700 years BP; (2) clayey silts (Fig. 1, Facies B) are included in a transgressive system tract, with tidal flat deposits overlain by open-bay sediments indicating a rapid rise of sea level between 8700 and 7000 years BP; (3) the upper lithofacies (Facies C to Facies F) record a regressive system tract coinciding with a still stand in the sea level (Goy and others 1996), which comprises the bulk of the valley fill.

Geochemistry

Four element associations may be recognized in the Spearman algorithm matrix (Table 4) and the PCA (Table 5). The highest abundances of the association 1 (SiO₂ up

to 80%) are found in the coarser sediments (fine to medium sands and gravels), indicating a grain size control in their distribution. By far the greatest concentrations of the association 2 (Factor 1: Al₂O₃-TiO₂-K₂O-MgO-Na₂O-P₂O₅-Be-Sc-V-Cr-Co-Ni-Y-Zr-Ba) and association 3 (Factor 2: Fe₂O₃-MnO-Cu-Zn-As-Mo-Ag-Pb) were found in the upper five samples, this break being more acute in the association 3 (even two orders of magnitude) than in the association 2. Sandy sediments are characterized by low concentrations of both groups. Association 4 (Factor 3: CaO-Sr-LOI-MgO) is present in significant quantities (up to 25%) in the Neogene deposits. The moderate contents observed in some estuarine samples (5–10%) may be related to the abundance of biogenic components, mainly shells of marine mollusks.

Some significant differences may be observed between the three clusters (Table 6). Cluster 1 includes Neogene and Holocene fine, noncontaminated sediments and, taking into account that unpolluted silts and clays of others adjacent estuaries and the Atlantic shelf have a bulk metal content very close to the mean of this group (Borrego 1992; González-Regalado and others 1996; Ruiz Muñoz

Table 6
Partition of 20 sediment samples to three clusters

cluster 1: samples 6-7-8-13-14-15-18-19-20
cluster 2: samples 1-2-3-4-5
cluster 3: samples 9-10-11-12-16-17

element	cluster 1		cluster 2		cluster 3	
	mean	max-min	mean	max-min	mean	max-min
%						
SiO ₂	59.5	74.2 - 43.5	53.0	65.4 - 45.9	85.6	90.6 - 71.7
Al ₂ O ₃	10.5	12.4 - 8.3	15.1	18.7 - 10.1	3.8	4.5 - 2.6
Fe ₂ O ₃	4.5	5.4 - 3.0	11.3	16.6 - 7.6	1.7	2.5 - 0.7
MnO	0.04	0.08 - 0.03	0.06	0.10 - 0.05	0.02	0.03 - 0
CaO	7.9	15.7 - 2.2	1.2	1.4 - 0.9	3.0	10.2 - 0.4
TiO ₂	0.66	0.78 - 0.58	0.86	1.01 - 0.69	0.25	0.36 - 0.16
K ₂ O	1.84	2.25 - 1.35	2.35	3.00 - 1.59	0.89	1.26 - 0.58
Na ₂ O	1.39	1.99 - 0.81	1.92	2.18 - 1.52	0.75	0.87 - 0.54
P ₂ O ₅	0.01	0.15 - 0.06	0.14	0.17 - 0.09	0.04	0.06 - 0.03
LOI	12.0	19.2 - 6.1	12.5	15.5 - 7.6	3.6	9.9 - 1.5
mg/kg						
Be	0.8	1.0 - 0.6	1.3	1.5 - 1.0	0.2	0.2
Sc	2.6	3.2 - 1.9	5.3	7.0 - 3.1	0.6	1.0 - 0.2
V	25	31 - 21	55.8	65 - 39	10.8	14 - 6
Cr	21.1	24 - 17	38.0	48 - 23	8.5	13 - 5
Co	6.8	9 - 5	13.0	18 - 8	4.2	6 - 3
Ni	12.4	17 - 8	19.8	28 - 11	4.2	8 - 0.5
Cu	13.0	19.4 - 8.1	612	933 - 175	13.1	40 - 3.8
Zn	39.0	47.3 - 29.4	706	1370 - 170	15.9	27.3 - 6.3
As	7.3	13.0 - 1.5	356	697 - 50	6.8	13.0 - 1.5
Y	6.5	8.2 - 4.8	10.5	12.9 - 7.2	2.3	2.9 - 1.4
Zr	6.6	8.1 - 5.2	7.6	9.0 - 5.3	3.9	4.6 - 3.0
Mo	1.4	3.0 - 0.5	7.4	11.0 - 3.0	1.7	3.0 - 0.5
Ag	0.4	0.8 - 0.1	1.2	1.8 - 0.8	0.4	0.7 - 0.1
Ba	7.6	9.2 - 6.0	12.0	16.5 - 7.5	3.6	4.3 - 2.2
Pb	15.4	51 - 5	151	234 - 81	4.3	11 - 1

and others 1996, 1997), it is reasonable to assume that mean values of trace elements (mainly the associations 2 and 3) of this class may be considered as a regional background of this type of sediments. This mean will be utilized to evaluate the metal pollution of some estuarine environments such as salt marshes, channel margin, or tidal flats.

Cluster 2 comprises the five upper samples, which include the last 2 m of natural filling (samples 3, 4, and 5). This group may be easily separated by their high metal pollution (associations 2 and 3). Sample 5 (4.5 m depth) shows a first metal enrichment in relation to the lower samples; this break indicates the evidence of the initial industrial mining between 2800 and 1800 years BP (Phoenician and Roman phases). Metal contents of sample 4 (4 m depth) are similar and may be interpreted as a consequence of the interruption in the mining activities during the Arabic domination. The higher metallic concentrations of the borehole were determined in sample 3, taken at 3.3 m depth. This very polluted layer (0.3–0.4 m width) has been found in other cores collected in the Tinto-Odiel Estuary and was deposited in the last decades (Borrego 1992; González-Regalado and others 1996). The metal concentrations (in mg/kg) of the Guadiana estuary, one unpolluted area located near the Tinto-Odiel estuary, are very low (Cu: 9–103; Zn: 74–180; Pb: 9–39) in comparison with the metal levels detected in this layer (Ruiz Muñoz and others 1996).

The upper 3 m belong to an anthropogenic filling with recent surface sediments dredged in the main channel of the Odiel River and wastes from saltworks located north of Bacuta Island. Fernández and others (1997) obtained similar metallic contents analyzing the bulk metal content of the subtidal sediments of the estuary mouth. Cluster 3 comprises the two unpolluted sandy layers of the borehole, with a mean which may be utilized as background for some estuarine and marine environments with similar grain size distribution, such as the main channels, fluvial bars, beaches, or shallow marine sediments.

In conclusion, two backgrounds may be obtained for pre-mining sandy and silty-clayey sediments, respectively. The concentration of heavy metals supplied by historic mining activities is lower than the industrial contamination because of the very high metal content determined in the upper natural layer (3.0 to 3.3 m depth) of the borehole, which was deposited during the last forty years.

References

- ALLEN GP, POSAMENTIER HW (1993) Sequence stratigraphy and facies model of an incised valley fill: the Gironde Estuary, France. *J Sediment Petrol* 63:378–391
- A.M.A. (Agencia del Medio Ambiente) (1994) Informe Esturién. Preliminary report vol 1
- ANDERBERG MR (1973) Cluster analysis for applications. Academic Press, New York
- BLANCO FREIJERO A, ROTHENBERG B (1981) Exploración arqueometalúrgica de Huelva. Labor, Barcelona
- BORREGO J (1992) Sedimentología del estuario del río Odiel. Ph D thesis, Univ of Seville
- BORREGO J, MORALES JA, PENDÓN JG (1993) Holocene filling of an Estuarine Lagoon along the Mesotidal Coast of Huelva: the Piedras River Mouth, southwestern Spain. *J Coast Res* 9:242–254
- BORREGO J, MORALES JA, PENDÓN JG (1995) Holocene estuarine facies along the mesotidal coast of Huelva, south-western Spain. In: Flemming BW, Bartholomä A (eds) Tidal signatures in modern and ancient sediments. *Spec Publ Int Ass Sedimentology* 24:151–170
- CABRERA F, CONDE B, FLORES V (1992) Heavy metals in the surface sediments of the tidal river Tinto (SW Spain). *Fresenius Environ Bull* 1:400–405
- CIVIS J, SIERRA FJ, GONZÁLEZ DELGADO JA, FLORES JA, ANDRÉS I, PORTA J, VALLE MF (1987) El Neógeno marino de la provincia de Huelva: antecedentes y definición de las unidades litoestratigráficas. In: Univ Salamanca (ed) Paleontología del Neógeno de Huelva (W. Cuenca del Guadalquivir), pp 9–23
- DALRYMPLE RW, ZAITLIN BA, BOYD R (1992) Estuarine facies models: conceptual basis and stratigraphical implications. *J Sediment Petrol* 62:1130–1146
- FERNÁNDEZ JC, RUIZ F, GALÁN E (1997) Clay mineral and heavy metal distributions in the lower estuary of Huelva and adjacent Atlantic shelf, SW Spain. *Sci Total Environ* 198:181–200
- FERRERO MD (1988) Los conflictos de Febrero de 1888 en Riotinto. Huelva en su Historia 2:603–623
- GONZÁLEZ-REGALADO ML, RUIZ MUÑOZ F, BORREGO J (1996) Evolución de la distribución de los foraminíferos bentónicos en un medio contaminado: el estuario del río Odiel (Huelva, SO España). *Rev Esp Paleontol* 11:1–10
- GOY JL, ZACO C, DABRIO CJ, LARIO J, BORJA F, SIERRA F, FLORES JA (1996) Global and regional factors controlling changes of coastlines in southern Iberia (Spain) during the Holocene. *Q Sci Rev* 15:773–780
- I.E.O. (Instituto Español de Oceanografía) (1982) Estudio de la contaminación en la ría de Huelva. Informe final Internal report
- I.E.O. (Instituto Español de Oceanografía) (1992) Variación espacio-temporal de parámetros físico-químicos y biológicos en la ría de Huelva y área de influencia, en el periodo 1987–1991. Internal report no 138
- M.O.P.U. (Ministerio de obras Públicas y Urbanismo) (1982) Estudio de la contaminación de la ría de Huelva. Evaluación de vertidos, planes, usos y actividades en la zona de influencia. Diagnóstico de la situación actual de marismas y esteros. Internal report
- NELSON CH, LAMOTHE PJ (1993) Heavy metals anomalies in the Tinto and Odiel River and Estuary System, Spain. *Estuaries* 16:496–511
- PÉREZ M, USERO J, GRACIA I, CABRERA F (1991) Trace metals in sediments from the “Ría de Huelva”. *Toxicol Environ Chem* 31–32:275–283
- REYMENT RA, JORESOG KG (1993) Applied factor analysis in the natural sciences. Cambridge University Press, Cambridge
- RUBIO JC (1985) Ecología de las marismas del Odiel. PhD thesis, Univ of Seville
- RUIZ MUÑOZ F, GONZÁLEZ-REGALADO ML (1990) Los ostrácos del tramo inferior de la Formación “Arcillas de Gibraleón” (Gibraleón, provincia de Huelva Sw España). *Rev Soc Geol España* 3:23–30

- RIUZ MUÑOZ F, GONZÁLEZ-REGALADO ML, MORALES JA (1996) Distribución y ecología de los foraminíferos y ostrácodos actuales del estuario mesomareal del río Guadiana (SO España). *Geobios* 29:513–528
- RIUZ MUÑOZ F, GONZÁLEZ-REGALADO ML, MUÑOZ JM, FERNÁNDEZ JC (1997) Contaminación metálica en los sedimentos litorales del Norte del Golfo de Cádiz (SO de España). *Rev Soc Geol España* 10:113–121
- SERRANO J, VIÑAS L, LÓPEZ FERNÁNDEZ AJ (1995) Proyecto de regeneración de los ríos Tinto y Odiel (Huelva). *Tecnoambiente* 53:53–56
- ZAZO C, DABRIO CJ, GOY JI, BARDAJI T, GHALEB B, LARIO J, HOYOS M, HILLAIRE-MARCEL CL, SIERRO FJ, FLORES JA, SILVA OG, BORJA F (1996) Cambios en la dinámica litoral y nivel del mar durante el Holoceno en el Sur de Iberia y Canarias Orientales. *Geogaceta* 20:1679–1682